

Received 22 October 2023, accepted 20 November 2023, date of publication 24 November 2023, date of current version 1 December 2023.

Digital Object Identifier 10.1109/ACCESS.2023.3336860

RESEARCH ARTICLE

In-Air Signature Verification System Based on Beta-Elliptical Approach and Fuzzy Perceptual Detector

ABDULAZEEZ R. ALOBAIDI^{1,2}, **THAMEUR DHIEB**^{1,3}, (Member, IEEE),
TAREK M. HAMDANI^{1,4}, (Senior Member, IEEE), **ALI WALI**^{1,5}, (Senior Member, IEEE),
KHMAIES OUAHADA^{1,6}, (Senior Member, IEEE), AND
ADEL M. ALIMI^{1,6}, (Senior Member, IEEE)

¹Research Groups in Intelligent Machines (REGIM Laboratory), National Engineering School of Sfax (ENIS), University of Sfax, Sfax 3038, Tunisia

²Department of Computer Techniques Engineering, Faculty of Information Technology, Imam Ja'afar Al-Sadiq University, Baghdad 10001, Iraq

³Higher Institute of Business Administration, University of Gafsa, Gafsa 2112, Tunisia

⁴Higher Institute of Computer Science Mahdia, University of Monastir, Mahdia 5111, Tunisia

⁵Higher Institute of Computer Science and Multimedia of Sfax, University of Sfax, Sfax 3000, Tunisia

⁶Department of Electrical and Electronic Engineering Science, University of Johannesburg, Auckland Park, Johannesburg 2006, South Africa

Corresponding author: Abdulazeez R. Alobaidi (abdulazeez.riyadh@sadiq.edu.iq)

This work was supported in part by the Tunisian Ministry of Higher Education and Scientific Research under Grant LR11ES48 and in part by the University of Johannesburg.

This work involved human subjects in its research. Approval of all ethical and experimental procedures and protocols was granted by the Sfax University Ethics Committee and performed in line with the Declaration of Helsinki.

ABSTRACT Believing that biometrics trends are moving to distant and contactless mode, in-air signature verification is nowadays considered as one of the principal users biometric identification in contactless mode allowing users identification by drawing their handwritten signature in the air. In-air signature verification is used in many applications like access control and forensic analysis. In this regard, we propose a novel system for in-air signature verification using Beta stroke segmentation. The Beta-elliptical approach and the fuzzy perceptual detector are used for features extraction. The proposed system defines a specific data acquisition protocol and uses preprocessing steps to prepare data. Finally, the verification phase is done based on Dynamic Time Warping. To evaluate our proposed system, we have created two in-air signature datasets with and without the use of a transparent glass plate, which we make publicly available at <https://iee-dataport.org/documents/air-signature-databases>, termed respectively In-Air Signature dataset (IAS dataset) and In-Air Signature dataset using Glass Plate (IASGP dataset). Our verification system demonstrates promising outcomes, yielding an Equal Error Rate (EER) of 1.25% when applied to the IAS dataset and an EER of 2.00% when applied to the IASGP dataset in the skilled-forgery scenario. Extensive evaluations were conducted on both the 3DAirSig and the DeepAirSig datasets. The results confirm that the proposed system has a good performance compared to existing in-air signature verification systems for both skilled-forgery and random-forgery scenarios.

INDEX TERMS In-air signature verification, beta-elliptical approach, fuzzy perceptual detector, dynamic time warping.

I. INTRODUCTION

A. BACKGROUND

Biometric-based personal verification methods leverage individuals' inherent characteristics, avoiding the drawbacks

The associate editor coordinating the review of this manuscript and approving it for publication was Junggab Son¹.

associated with token or knowledge-based approaches such as ID cards or passwords, which can be lost, stolen, or forgotten [1]. The signature is one of the most biometric personality traits that can be acceptable legally [2]. A person's signature exhibits distinct behavioral characteristics, making it a de facto identifier. One of the primary benefits of signature biometrics lies in its user-friendliness. Signature

identification identifies the signature's owner, whereas signature verification that we will focus on in this paper finds whether a signature is genuine or forged [3]. The research in the field of signature verification increased in the last years [4]. Many applications use signature verification systems like mail voting, access controls, official communications, forensic analysis and banking services [5], [6].

Traditionally, researchers tend to treat individual verification based on their signatures as two distinct types namely offline and online. In the offline type, only the image of the signature path is available [7]. Whereas, in the online type, data comprise information about the pen movement of the signature over time, besides, other physical measurements, are available [8]. Due to the covid-19 situation, people prefer to not touch any screen devices because the latter can cause many infectious disease viruses. Consequently, contactless systems are emerging based on hygiene and maintenance reasons [9]. For this reason, the in-air signature verification is spreading these days. In-air signatures are a new modality that permits a person to sign in the air by allowing free hand movements, that way dispensing with the use of a signing surface. Compared to offline and online signature verification, in-air signature verification systems have not yet reached maturity [10]. Therefore, analyzing in-air signatures has been taken as the base modality of the present research work.

Indeed, in-air signature verification has posed real difficulties and challenges. One of the greatest challenges is the task of fingertip tracking. Therefore, it is difficult to get the correct path of the signature in the air. In addition, the occlusions of fingers and the viewpoint changes during signing freely in the air can affect the in-air signature verification systems' accuracy. Another difficulty with in-air signature verification is the factor that forgeries can be highly skillful as the other types of signatures. The limited number of reference signatures per signer represents another difficulty [11]. Moreover, the neurophysiological characteristics (e.g. muscle strength and nervous system) and the psychological characteristics of an individual (e.g. stress and apprehension) influence the signature of the person. For example, because of the variability of the in-air signature speed, the same individual can have two signatures with dissimilar path distances. Thus, the person in a certain case is not able to provide a particular biometric. Consequently, an important challenge associated with in-air signature verification systems is to determine a set of characteristics able to represent the in-air signatures well.

B. CONTRIBUTIONS

Our proposed system aims to overcome the mentioned difficulties and challenges. Firstly, to get the correct path of the signature in the air even if the viewpoint changes during the signing, we will incorporate the MediaPipe Hands framework [12] into our work, offering accurate finger and hand tracking capabilities. Secondly, in order

to well characterize the in-air signature, we will use the Beta-elliptical approach [13], [14] and the fuzzy perceptual detector [15], [16]. Finally, to tackle the issue of having a limited number of reference signatures for each signer, we will utilize the Dynamic Time Warping algorithm (DTW). In fact, DTW plays a crucial role in this context as it offers a robust solution for aligning and comparing time-series data, allowing us to effectively analyze and verify signatures even with minimal reference samples.

Our contributions can be summarized as follows:

- Two in-air signature datasets are created and publicly published with and without using a transparent glass plate. Each one contains 400 in-air signatures entered by 40 subjects.
- The Beta strokes segmentation is applied to segment the in-air signatures trajectory.
- The Beta-elliptical approach and the fuzzy perceptual detector are adopted for the first time in the features extraction to the in-air signature verification system.
- The proposed system which employs publicly accessible datasets, is illustrated and proves its superiority over existing methods.

C. PAPER ORGANISATION

The rest of the paper is organized as follows. Section II describes the related works of in-air signature verification systems. In Section III, our proposed datasets will be thoroughly presented. Section IV describes the methodology of the proposed system. The experimental setup and the performance evaluation are presented in Section V. Finally, in Section VI, conclusions and future works are discussed.

II. RELATED WORKS

Recently, with the widespread occurrence of an infectious disease in a community like the COVID-19 pandemic, various stone measures have been implemented to decrease the propagation of the virus. As a part of efforts, the predilection for touchless technology has been emerging [17], [18], [19]. Consequently, many researchers have proposed the use of in-air signature verification systems in many real-life applications. Among these, we can cite the in-air signature verification system presented in [20]. In this system, Ferrer et al. introduced a framework for the generation of synthetic 3D in-air signatures. This framework leverages the lognormality principle, which accurately replicates the intricate neuromotor control processes involved as the fingertip is in motion. To evaluate their system, the authors used real data and synthetic 3D signatures from Sigma-Lognormal model with DTW verification.

In [21], Diaz et al. presented a solution involving the synthesis of 3D signatures. In the initial stage, they focused on synthesizing the kinematics of 3D signatures drawing from the Kinematic Theory of Rapid Movements and the associated Sigma-Lognormal model in 3D. In the second stage, they extracted the velocity, the acceleration and

the three position coordinates. Finally, they performed the evaluation using the DTW algorithm.

Li et al. [10] proposed the use of Siamese's recurrent neural networks to characterize signatures and to determine whether an in-air signature is from the claimed user or an imposter. To evaluate their system, the authors created a new in-air dataset using smartwatch motion sensors collected from 22 individuals. The obtained results indicate the usefulness of the proposed system.

Khoh et al. [22] used hand detection and localization algorithms to extract the region of interest from each of the depth in-air signature images. Then, the authors extracted several vector-based features. Finally, the support vector machine was used in the verification phase.

Malik et al. [23] propose three different features of the signature trajectory namely spatial(X,Y), depth(Z) and 3D(X,Y,Z). For classification, they used DTW, Image-based verification, and PointCloud-based verification. The latter method outperforms all the compared algorithms using their created dataset called DeepAirSig dataset.

Okawa et al. [24] suggested a new system improving signature verification. In features extraction, they used X and Y coordinates, pressure, path-tangent angle, path velocity magnitude, log curvature radius and total acceleration magnitude. In addition, they proposed a novel single-template strategy using mean templates and DTW by the local stability sequence (LS-DTW). Their system was evaluated, in both the random and the skilled forgery scenarios using two public online signature datasets, SVC2004 Task 2, MCYT 100, and using the 3DAirSig dataset. The obtained results demonstrate the effectiveness of the proposed system.

Khoh et al. [25] proposed a novel in-air hand gesture signature verification in order to study the feasibility of transfer learning in classifying a hand gesture-based signature. To release their system, the authors detected and segmented the hand region from each depth image. After that, they extracted the salient spatial and temporal features from various images. For classification, they used AlexNet model.

Guerra-Segura et al. [26] proposed a novel in-air signature verification system using a Leap Motion controller to characterize in-air strokes. To evaluate their system, they created a new database collected from 100 individuals, which consists of 10 genuine signatures from each user and 10 forgeries for every original user. The extracted features are the mean which represents the absolute value generated by the distribution, its standard deviation, correlation, Shannon entropy, Kurtosis and Skewness. For classification, they used Least Square Support Vector Machine.

Khoh et al. [27] proposed a palm detection and a predictive palm segmentation algorithm to segment the palm region from the frame sequence. Then, they applied a two-dimensional representation of hand gesture signature based on a Motion History Image. The features have been extracted from this motion image subsequently. Lastly, the features matching was done using Euclidean distance, cosine distance,

chi-square distance, and Manhattan distance in order to calculate the dissimilarity score of a test sample.

To verify a test of in-air signature as being genuine or forged, Malik et al. [28] propose four features extraction methods which are:

- 1) Depth-based Signature Verification method (DSV) based on the 1D depth Z of the signature trajectory.
- 2) 2D Spatial-based Signature Verification method (SSV) based on the 2D spatial (X, Y) feature.
- 3) Improved 2D Spatial-based Signature Verification method (ISSV) based on the Spatial (X, Z) and Spatial (Y, Z).
- 4) 3D Signature Verification method (3D-SV) based on the 3D information altogether (X, Y, Z).

For the verification process, the authors used the multidimensional dynamic time warping algorithm. The evaluation was made on their own public dataset which consists of 600 signatures performed by 15 volunteers.

Fang et al. [29] presented a new video-based system for in-air signature verification. To do their system, the authors firstly used fingertip tracking in order to generate the trajectory of signature from the in-air signing videos. Secondly, they proposed an improved dynamic time warping algorithm, and they proved the validity of the Fast Fourier Transform technique in the field of track signature verification. Finally, they explored the feasibility of the fusion of the dynamic time warping algorithm with the Fast Fourier Transform technique based on Gaussian probability distribution. Table 1 summarizes recent works on in-air signature verification.

In reviewing the presented related works, several technical gaps and shortcomings emerge, which have motivated the design of our proposed methodology. In fact, in-air signature verification involves analyzing dynamic and continuous hand movements, and existing approaches often struggle to account for the natural variability in individual handwriting styles and speeds. The techniques rely on simplistic feature representations, which may not capture the intricate nuances of in-air signatures, potentially leading to accuracy issues. Moreover, achieving interoperability with various hardware devices and platforms is a challenge in in-air signature verification. Compatibility issues can hinder the adoption of such systems. The proposed methodology aims to bridge these technical gaps by offering a more comprehensive solution that addresses the complexities of in-air signature verification and improves user acceptance, making it a valuable contribution to this evolving field.

In the realm of in-air signature verification systems, a significant challenge lies in defining a set of features capable of effectively discriminating between genuine and forged in-air signatures of individuals. In this study, we investigate the effectiveness of employing the Beta-elliptical approach and the fuzzy perceptual detector for feature extraction in the context of in-air signature verification. To the best of our knowledge, the Beta-elliptical approach and the fuzzy perceptual detector have not been previously used for in-

TABLE 1. Summaries of recent works on in-air signature verification.

Ref	Year	Feature extraction	Verification	Performance	Dataset
[20]	2023	Sigma-Lognormal model	DTW	1.91% EER for skilled forgery and 0.27% EER for random forgery	DeepAirSig: contains the signatures of 40 individuals (a total of 1800). Material used: Intel's creative senz3D depth camera
[21]	2022	The velocity, the acceleration and the three position coordinates	DTW	5.09% EER for skilled forgery and 0.69% EER for random forgery	DeepAirSig: contains the signatures of 40 individuals (a total of 1800). Material used: Intel's creative senz3D depth camera
[10]	2022	Temporal sequential data	Siamese RNN	0.83% EER	Signature dataset: contains the signatures of 22 individuals (a total of 440). Material used: smartwatch motion sensors.
[22]	2022	Several vector-based features	Support vector machine	5.07% EER for skilled forgery 2.41% EER for random forgery	iHGS database: contains 2000 genuine signatures of 100 individuals and 980 forgery samples. Material used: a Microsoft Kinect sensor camera.
[23]	2020	Three different features of the signature trajectory namely spatial (X,Y), depth (Z) and 3D (X,Y,Z)	PointCloud-based verification	0.05% EER for skilled forgery	DeepAirSig: contains the signatures of 40 individuals (a total of 1800). Material used: Intel's creative senz3D depth camera
[24]	2018	X and Y coordinates, pressure, path-tangent angle, path velocity magnitude, log curvature radius and total acceleration magnitude	Mean templates and DTW	0.60% EER for skilled forgery and 0.57% EER for random forgery	3DAirSig: contains the signatures of 15 individuals (a total of 600). Material used: Three GoPro cameras.
			Mean templates and a weighted DTW	0.10% EER for skilled forgery and 0.57% EER for random forgery	
			Mean templates and sliding window DTW	0.10% EER for skilled forgery and 0.57% EER for random forgery	
			A novel single-template strategy using mean templates and DTW weighted by the local stability sequence	0% EER for skilled forgery and 0.52% EER for random forgery	
[25]	2018	XY, XT and YT plane projection from an image sequence, 3-layer XY plane projection with 0, 0.3 and 0.5 ratio, and Combination of 3 plane projections	AlexNet model	4.88% EER for skilled forgery and 0.87% EER for random forgery	HGS database: contains the signatures of 100 individuals (a total of 2000). Material used: a Microsoft Kinect sensor camera.
[26]	2021	The absolute value generated by the distribution, its standard deviation, correlation, shannon entropy, kurtosis and skewness	Least Square Support Vector Machine	0.25% EER for skilled forgery	Dataset contains the signatures of 100 individuals. Material used: a Leap Motion.
[27]	2019	X and Y profiles summation, concatenation of X-profile and Y-profile summations, Histogram of Oriented Gradient (HOG)	Euclidean distance, cosine distance, chi-square distance, and manhattan distance	3.22% EER for skilled forgery	HGS database: contains the signatures of 100 individuals (a total of 2000). Material used: a Microsoft Kinect sensor camera.
[28]	2018	DSV based on the 1D depth Z of the signature trajectory SSV based on the 2D spatial (X, Y) feature ISSV based on the Spatial (X, Z) and Spatial (Y, Z) 3D-SV based on the 3D information altogether (X, Y, Z)	Multidimensional dynamic time warping algorithm	0.51% EER for skilled forgery 0.69% EER for skilled forgery 0.58% EER for skilled forgery 0.46% EER for skilled forgery	3DAirSig: contains the signatures of 15 individuals (a total of 600). Material used: Three GoPro cameras
[29]	2017	Fast Fourier Transform technique	DTW	1.90% FAR 2.86% FRR for skilled forgery	Dataset contains the signatures of 14 individuals (a total of 560). Material used: high-speed camera.

TABLE 2. Characteristics of the participants in data collection.

Total number of samples collected	40
Men	31
Women	9
Right hand	32
Left hand	8
Age	21-23 10
	24-27 8
	28-30 8
	31-35 7
	36-40 7

air signature verification system. Our choice of using the Beta-elliptical approach and the fuzzy perceptual detector justified by the fact that these models are characterized by several types of information that is to say several features that can be used to well describe the signer. Moreover, we are interested in using Dynamic Time Warping in the verification phase. More details about our in-air signature datasets and our proposed verification system are presented in the next sections.

III. PROPOSED IN-AIR SIGNATURE DATASETS

Indeed, there is a lack of in-air signature datasets available for researchers [28]. The existing datasets employ various devices like the Leap Motion and the Microsoft Kinect sensor camera. However, these devices are not without their drawbacks and have certain limitations. Challenges include the expenses associated with their implementation, the need for technical expertise to operate them, and potential difficulties for users in adjusting their finger movements to fit within the device's restricted field of view, especially if they lack familiarity with such equipment.

To mitigate these issues, we have created two in-air signature datasets exclusively using a laptop's camera, eliminating the necessity for any additional specialized equipment. we make our new created datasets publicly available at <https://iee-dataport.org/documents/air-signature-databases>.

Forty participants voluntarily took part in each of the two datasets' construction. Written informed consent was obtained from each participant. Their age ranged from 21 to 40 years. Table 2 shows the characteristics of the participants in data collection.

Each volunteer signs five signatures in the air and imitates five signatures of five other volunteers in one session. We choose to take only five signatures to make in-air verification more challenging. Moreover, in real life generally, we take only a few signatures of users in the applications. Table 3 presents a short description of the constructed datasets.

The proposed protocol for data acquisition consists of two ways for the two in-air signature datasets respectively. In IAS dataset, the volunteer signs in the air directly in front of the camera. In IASGP dataset and in order to make the task of in-air signature verification more challengeable,

TABLE 3. Details of our in-air signature datasets.

Dataset	Signature type	Number of signatures
In-Air Signature dataset (IAS dataset)	Genuine	200
	Skilled forgeries	200
In-Air Signature dataset using Glass Plate (IASGP dataset)	Genuine	200
	Skilled forgeries	200

the volunteers sign in the air using a transparent glass plate between them and the camera.

A. IN-AIR SIGNATURE DATASET (IAS DATASET)

During data acquisition, volunteers were seated in a comfortable chair directly in front of the camera leaving a distance of 60 cm between their dominant hand and the camera. The volunteers were asked to raise their dominant hand in front of the camera. After that, they were asked to close all the fingers of the hand leaving only the index finger. Then they were asked to sign in the air. When the in-air signature is over, the volunteers were asked to open all the fingers of the used hand. The purpose of this protocol is to control the beginning and the end of the signature in the air for each volunteer.

To assure that the volunteers had accurately comprehended the demanded task, the experimenter performed the task. The volunteers were permitted to realize the requested task before the recording of the data for five minutes. The volunteers were asked to sign in the air at their preferred speed. Custom-made software was developed in Python using the MediaPipe Hands framework, offering accurate finger and hand tracking capabilities, to record the data on two files:

- The first file is a CSV file that contains the 2D coordinates of the signature in the air ($x(t)$ and $y(t)$).
- The second is an image file of the signature in the air.

Figure 1 shows an example of data acquisition for IAS dataset collected from the first author of this paper.

B. IN-AIR SIGNATURE DATASET USING GLASS PLATE (IASGP DATASET)

The experimental protocol for IASGP dataset acquisition is the same as in IAS dataset. The only difference is that we put a transparent glass plate in front of the camera, away 30 cm. This glass plate, with dimensions of 60 cm in both length and width, is placed inside a wooden frame and fixed on the table in front of the volunteers as shown in Figure 2.

During the in-air signature task, the volunteers touch the transparent glass plate in front of the camera. Figure 3 shows an example of data acquisition for IASGP dataset.

Figure 4 presents some examples of in-air signatures extracted from IAS and IASGP datasets. We can note that the forged in-air signatures in (B) and in (D) have more tremors than the genuine in-air signatures in (A) and (C) respectively. Moreover, the forged in-air signature in (B) extracted from IAS dataset without the use of a transparent glass plate has few tremors compared to the forged in-air signature in (D)

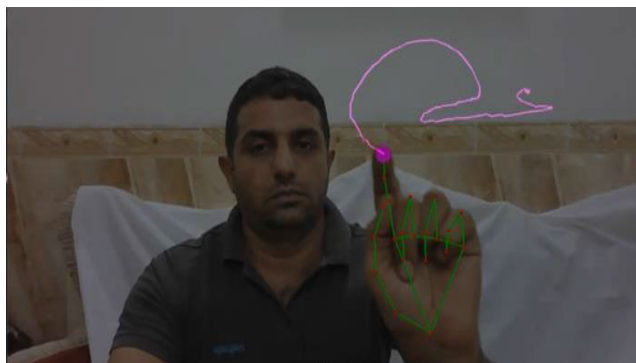


FIGURE 1. Example of data acquisition for IAS dataset.



FIGURE 2. Experimental setup using the transparent glass plate.



FIGURE 3. Example of data acquisition for IASGP dataset.

extracted from IASGP dataset with the use of a transparent glass plate.

IV. PROPOSED IN-AIR SIGNATURE VERIFICATION

The proposed methodology for in-air signature verification builds upon several foundational methods and techniques from the field of biometrics and pattern recognition. Here are the key methods that serve as the foundation for the design and development of the proposed methodology:

1) Data preprocessing: Robust data preprocessing steps are applied to address issues related to noise. Techniques such as normalization and Chebyshev type 2 filter are utilized to enhance data quality.

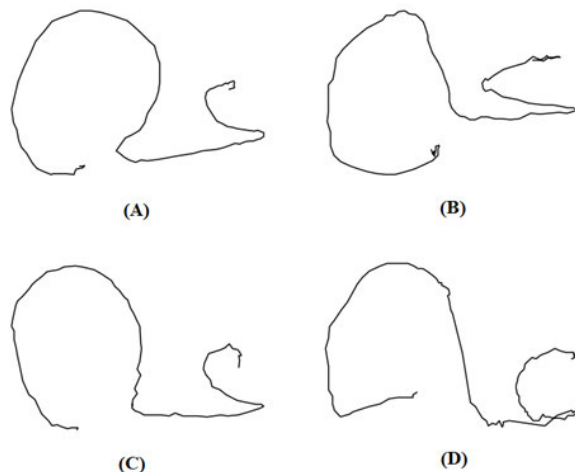


FIGURE 4. Examples of in-air signatures extracted from IAS and IASGP datasets for the same user. (A): genuine in-air signatures extracted from IAS dataset; (B): forged in-air signatures extracted from IAS dataset; (C): genuine in-air signatures extracted from IASGP dataset; (D): forged in-air signatures extracted from IASGP dataset.

2) Segmentation: Data segmentation step is applied to divide the in-air signature into Beta strokes.

3) Features extraction techniques: The methodology incorporates advanced features extraction techniques based on Beta-elliptical approach and fuzzy perceptual detector. These methods aim to capture the salient information from the dynamic in-air signature trajectories.

4) Dynamic Time Warping (DTW): DTW is used as a similarity measure to compare the in-air signature trajectories. DTW helps account for variations in signature execution speed and timing, making it a crucial component for accurate verification.

5) Decision threshold: To establish an appropriate threshold for verification, threshold selection algorithms like Equal Error Rate (EER) optimization are integrated into the methodology. This algorithm helps determine the decision boundary between genuine and forgery samples.

The main components of the proposed system are shown in Figure 5.

A detailed explanation of the proposed system components will be presented in the following sub-sections.

A. PREPROCESSING

The input of our in-air signature verification system is the coordinates in time of the index fingertip positions $x(t)$ and $y(t)$. To perform the preprocessing step, we have adjusted the vertical dimension h of the in-air signatures lines to obtain a normalized size to keep the original height-to-width ratio. The h value is set to 128 after many experimental tests. For each point of the hand movement trajectory, the normalization is done by computing its normalized coordinates x_{norm} and y_{norm} attained by the following

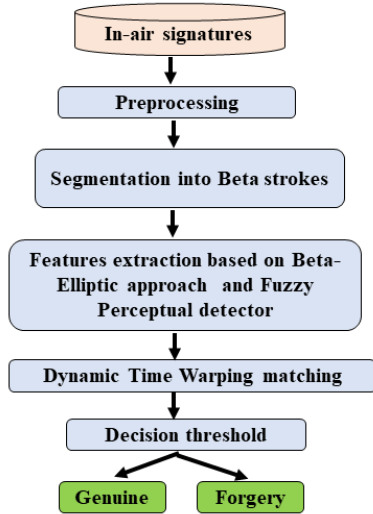


FIGURE 5. General architecture of the proposed in-air signature verification system.

formulas:

$$x_{norm} = h \cdot \frac{x - x_{min}}{m} \tag{1}$$

$$y_{norm} = h \cdot \frac{y - y_{min}}{m} \tag{2}$$

where

$$m = \max(\max_x - \min_x, \max_y - \min_y) \tag{3}$$

where (x,y) are the original point coordinates, x_{norm} and y_{norm} are the corresponding ones after the normalization procedure, and h is the value chosen to achieve the normalization.

Thereafter, a Chebyshev type 2 filter with a cut-off frequency equal to 12Hz is performed to eliminate the noise. The choice of using the Chebyshev type 2 filter among many filters is based on the following factors:

1) Chebyshev Type 2 filters are known for their variable ripple in the stopband, which means they can provide strong attenuation for certain frequencies while allowing others to pass with minimal distortion. Depending on the frequency characteristics of in-air signatures, this filter type is chosen to emphasize specific frequency components relevant to the task.

2) Since in-air signature signals deal with low Signal-to-Noise Ratio (SNR), Chebyshev Type 2 filters are preferred due to their ability to provide deep stopband attenuation, which can help reduce noise and interference from unwanted frequencies.

3) Chebyshev Type 2 filters offer flexibility in designing filter responses by adjusting parameters like the amount of ripple and the filter order. This allows designers to tailor the filter to the specific requirements of the in-air signature verification task, balancing the trade-off between passband ripple and stopband attenuation.

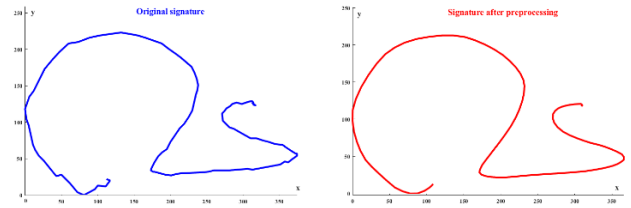


FIGURE 6. Application of preprocessing on an example of an in-air signature extracted from IAS dataset.

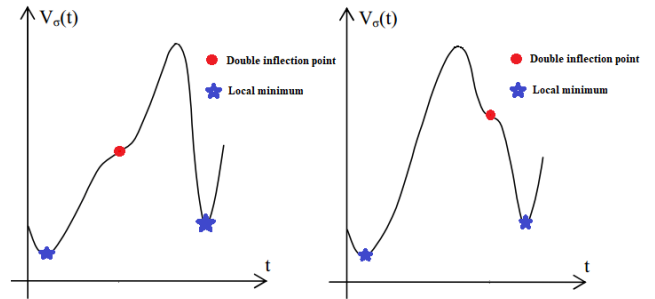


FIGURE 7. Detection of segmentation points from the curvilinear velocity profile.

Figure 6 shows an application of preprocessing to an in-air signature extracted from IAS dataset.

B. SEGMENTATION

To segment the in-air signatures, firstly, we represent the curvilinear velocity by the following equation:

$$V_{\sigma}(t) = \sqrt{\left(\frac{dx(t)}{dt}\right)^2 + \left(\frac{dy(t)}{dt}\right)^2} \tag{4}$$

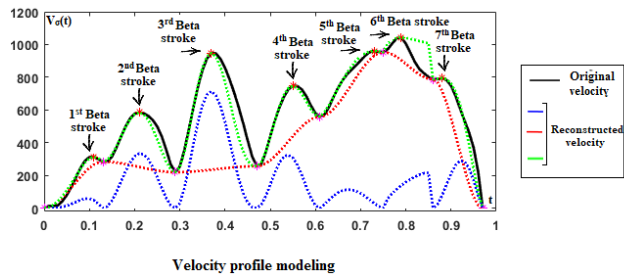
Afterward, we detect two types of points from $V_{\sigma}(t)$ as depicted in Figure 7 below, which are:

- The double inflection point represents the variation of speed that indicates the transition of the movement drive from a neuromuscular subsystem to another or from a neurophysiologic impulse to the following which corresponds to the change in convexity in the path.
- The local minimum represents the local minima of the curvilinear velocity.

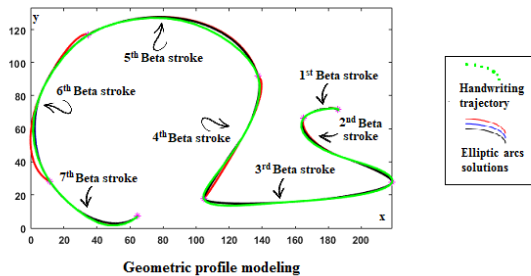
Thereafter, we divided the curvilinear velocity into small elements called Beta strokes delimited between two successive velocity local minimums or double inflection points. After that, we divided the in-air signature path into strokes delimited between the correspondents' points used in the curvilinear velocity segmentation. An example of segmentation of in-air signature extracted from IAS dataset is depicted in Figure 8.

C. FEATURES EXTRACTION

we are interested to use Beta-elliptical approach in the in-air signature verification system, which sufficiently represents



Velocity profile modeling



Geometric profile modeling

FIGURE 8. Segmentation of an example of an in-air signature extracted from IAS dataset.

the hand movements in real-time, by describing together its profile parts: the Beta impulses and the elliptic arcs [13], [14], [30]. Besides, we are interested to utilize the fuzzy perceptual detector in order to adequately represent the hand movements path [15], [16].

Hand movement is considered as the consequence of the activation of many neuromuscular subsystems performed by the neuronal system and transferred by the nerves motor to the muscles to activate the arm of the hand. The research done on the impact of these neuromuscular subsystems on the dynamic profile called also velocity profile indicates that each subsystem produces an impulsive signal converged to a Beta function [31] expressed as follows.

$$pulse \beta (K, t, q, p, t_0, t_1) = \begin{cases} K \cdot \left(\frac{t-t_0}{t_c-t_0}\right)^p \cdot \left(\frac{t_1-t}{t_1-t_c}\right)^q & \text{if } t \in [t_0, t_1] \\ 0, & \text{elsewhere} \end{cases} \quad (5)$$

where t_0 and t_1 denote respectively the start and the end times of the constructed impulse, t_c is the time when the impulse achieves its highest amplitude K , p and q are intermediate parameters. The velocity profile can be calculated as given in formula 6.

$$V(t) = \sum_{i=1}^n V_i (t - t_{0i}) = \sum_{i=1}^n pulse \beta_i (K_i, t, q_i, p_i, t_{0i}, t_{1i}) \quad (6)$$

Boubaker et al. [14] suggest a new method for modeling the velocity profile based on the Beta function with the addition of a continuous training component called Extended Beta-Elliptical model which we used in this work. In this model, the curvilinear velocity inside the interval time $[t_0, t_1]$ is divided into two elements:

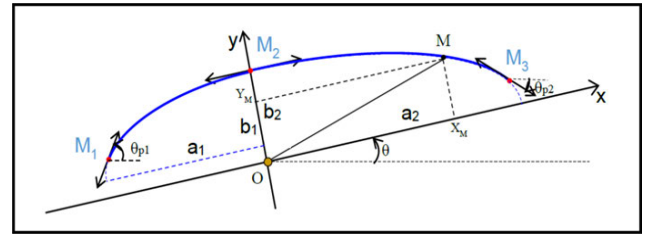


FIGURE 9. Parameters of the geometric profile.

1) AN IMPULSIVE ELEMENT AS DEPICTED IN (7)

$$V_{Imp}(t) = K \cdot \left(\frac{t-t_0}{t_c-t_0}\right)^p \cdot \left(\frac{t_1-t}{t_1-t_c}\right)^q \quad (7)$$

where t_0 and t_1 denote respectively the start and the end times of the constructed impulse, t_c is the time when the impulse achieves its highest amplitude K , p and q are intermediate parameters.

2) A CONTINUOUS TRAINING ELEMENT, CALCULATED USING (8)

$$V_{Tra}(t) = A \cdot \left[\frac{(t-t_0)^3}{3} - \frac{(t_1-t_0) \cdot (t-t_0)^2}{2} \right] + V_i \quad (8)$$

where

$$A = -6 \cdot \frac{V_f - V_i}{(t_1 - t_0)^3} \quad (9)$$

where:

- t_0 and t_1 denote respectively the start and the end times of the constructed impulse.

- V_i and V_f are respectively the velocities at the start and the end times of the constructed impulse.

Finally, the curvilinear velocity is the sum of the impulsive element and the continuous training element as defined in (10):

$$V_{R(t)} = V_{Imp}(t) + V_{Tra}(t) \quad (10)$$

In the geometric profile, each stroke can be fitted utilizing two adjacent elliptic arcs $E_1(a_1, b_1, \theta_1, \theta_{p1})$ and $E_2(a_2, b_2, \theta_2, \theta_{p2})$ as presented in Figure 9.

These two arcs have the same inclination angles ($\theta_1 = \theta_2 = \theta$). To guarantee the continuity of curvature when departing from the first to the second elliptic arc, the link between the two small and large axis lengths should confirm the condition shown in (11).

$$a_2 = a_1 \cdot \sqrt{\frac{b_2}{b_1}} \quad (11)$$

where:

- a_1 and a_2 are respectively the major axis half-length of the ellipse including the first arc and the second arc.

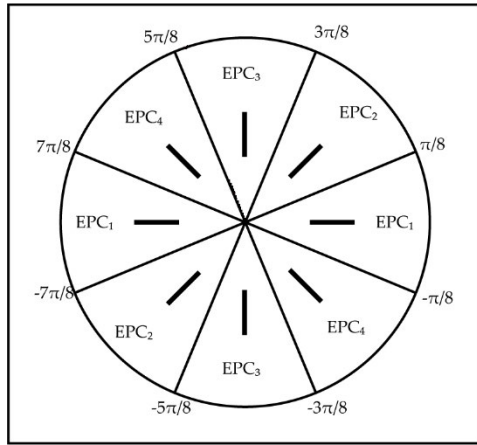


FIGURE 10. Presentation of EPCs on the trigonometric circle.

$-b_1$ and b_2 are respectively the small axis half-length of the ellipse supporting the first arc and the second arc.

In addition, we integrate into the features extraction phase the coefficient of logarithmic proportionality between the curvilinear velocity and the curvature radius λ known also as the two-thirds power law [32]. We compute this parameter as the average absolute gradient of the parametric curve describing the variation of the logarithm of the curvilinear velocity with respect to the logarithm of the curvature radius as expressed in (12):

$$\lambda = \frac{1}{N} \times \sum_{n=1}^N \left| \frac{\ln(V_\sigma(t_{n+1})) - \ln(V_\sigma(t_n))}{\ln(R_c(t_{n+1})) - \ln(R_c(t_n))} \right| \quad (12)$$

- where:

- N is the points number in the current stroke.
- n is the current index of points in the trajectory and t_n represents its execution time.

On the other hand and inspired by the PerTOHS theory (Perceptual Theory for On-line Handwriting Segmentation) [15], [16], we propose to use the fuzzy perceptual detector for our in-air signature verification system. Thus, we use the inclination angle of the ellipse major axis to attach each Beta stroke to one of the four types of Elementary Perceptual Codes (EPC) as shown in Table 4.

TABLE 4. Shape of EPC.

EPC	Designation	Shape
EPC ₁	Valley	
EPC ₂	Left oblique shaft	
EPC ₃	Shaft	
EPC ₄	Right oblique shaft	

We divide the trigonometric circle into eight regions corresponding to the EPC as displayed in Figure 10

Indeed, EPCs have a problem with ambiguity and indecision caused by several conditions such as hand disorder. To overcome this drawback, we used the fuzzy logic theory to assign a membership degree for each EPC. Therefore, we achieved four features which are FEPC₁, FEPC₂, FEPC₃, and FEPC₄ denoting respectively the membership degree of EPC₁, EPC₂, EPC₃, and EPC₄.

To recapitulate, each one of the Beta strokes is represented by 22 features as given in Table 5.

TABLE 5. Extracted features based on beta-elliptical approach and fuzzy perceptual detector.

N°	Feature	Description
1	$t_1 - t_0$	Duration of the Beta signal
2	$\frac{t_c - t_0}{t_1 - t_0}$	Report of the Beta signal asymmetry
3	P	Parameter of the Beta signal
4	K	Amplitude of the Beta signal
5	V_i	Velocity at the starting instant of the Beta signal
6	V_f	Velocity at the ending instant of the Beta signal
7	$\frac{k_i}{\text{training}}$	Report of the amplitude of Beta signal with respect to the medium value of the training component
8	a_1	Major axis half-length of the ellipse concerning the first arc
9	b_1	Small axis half-length of the ellipse concerning the first arc
10	b_2	Small axis half-length of the ellipse concerning the second arc
11	θ_{p1}	Inclination angle of the tangents at the endpoint M1
12	θ	Inclination angle of the ellipse major axis
13	FEPC1	EPC ₁ with membership degree value
14	FEPC2	EPC ₂ with membership degree value
15	FEPC3	EPC ₃ with membership degree value
16	FEPC4	EPC ₄ with membership degree value
17	θ_{p2}	Inclination angle of the tangents at the endpoint M3
18	Stroke position	Position of the Beta stroke in the in-air signature
19	$\theta_{\text{departure}}$	Inclination angle of departure
20	θ_{arrival}	Inclination angle of arrival
21	$\sum \Delta \theta$	Curvature angle of path stroke
22	λ	Coefficient of logarithmic proportionality between the curvilinear velocity and the curvature radius

The first seven features depict the neuromuscular excitations affected during the in-air signature actions while the fourteen following features express the geometric characteristics in the path of the in-air signatures. The last parameter allows a precise description of the shape of the path curvature radius variation in the in-air signatures.

D. VERIFICATION BASED ON DYNAMIC TIME WARPING

1) DYNAMIC TIME WARPING MATCHING

Dynamic Time Warping algorithm (DTW) is a well-known algorithm in numerous fields of research like gestures recognition [33], eye movement analysis [34], pattern recreation [35] and signature verification [4].

DTW permits a non-linear mapping of one time series to another by minimizing the distance between the two. Therefore, to calculate the distance between two in-air signatures, a simple design of the DTW algorithm is used, which can align two non-linear temporal sequences via dynamic programming. The distance matrix between a reference signature $R = \{r(i)\}_{i=1..N}$ described by N Beta strokes and a questioned signature $Q = \{q(j)\}_{j=1..M}$ described by M Beta strokes, can be computed by filling a $DTW_{N+1 \times M+1}$ matrix following equation (13) after initialization of $DTW[0, 0] = 0$ and $DTW[i, 0] = DTW[0, j] = \infty \forall i, j \in [1, N]$:

$$DTW[i, j] = dist(i, j) + \min \left\{ \begin{array}{l} dist(i-1, j) \\ dist(i, j-1) \\ dist(i-1, j-1) \end{array} \right\} \quad (13)$$

The distance between reference and questioned signatures will be saved at the upper right corner of the DTW matrix:

$$Dist(R, Q) = DTW(N, M) \quad (14)$$

Moreover, the local distance $dist$ in (13) was the usual Euclidean vector distance as shown in (15).

$$dist(f_i^R, f_j^Q) = \sqrt{\sum_{k=1}^{22} (f_{i,k}^R - f_{j,k}^Q)^2} \quad (15)$$

where k denotes the k^{th} feature dimension. Let us remember that 22 is the total number of extracted features.

2) SELECTION OF A TEMPLATE SIGNATURE

The DTW distances reflect in a way the similarity of a questioned signature with a reference genuine signature of a signer. For the training, we use G reference genuine signatures $\{S_1, S_2, \dots, S_G\}$ for each user. Thus, we compute the DTW distance between each one of the G reference genuine signatures with the remaining reference genuine signatures. Therefore, we choose one template genuine signature for DTW $S_{indexDTW}$ for that user as detailed in Algorithm 1.

Thus, only the signatures $S_{indexDTW}$ will be used in the distance measurement for the testing. Therefore, for the final verification decision, we calculate the distance measurement between the signatures $S_{indexDTW}$ and the questioned signature. If the distance measurement is inferior to a specific threshold, the questioned signature will be considered as genuine. Otherwise, the questioned signature will be considered forgery.

V. EXPERIMENTS AND DISCUSSION

A. EVALUATION PROTOCOL

We used three metrics to evaluate the performance of our in-air signature verification system which are:

- False Acceptance Rate (FAR) is the probability that forged in-air signatures are incorrectly accepted as genuine

Algorithm 1 Selection of Template Signature: $S_{indexDTW}$

G reference genuine signatures $\{S_1, S_2, \dots, S_G\}$

indexDTW = 0

minDTW = 100

For $k = 1: G$

$$DTWdistance(k) = \sum_{q=1}^N DTWdistance(S_k, S_q)$$

if (DTW distance(k) < minDTW)

minDTW = DTW distance(k)

indexDTW = k

end

end

return ($S_{indexDTW}$)

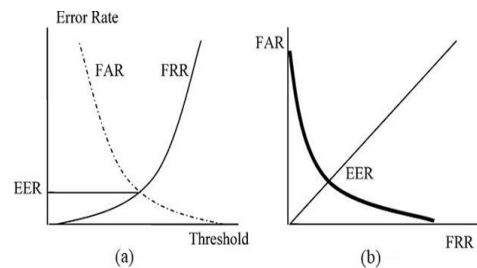


FIGURE 11. (a) Relationship between FAR, FRR and EER (b) ROC curve.

in-air signatures by the system.

$$FAR = \frac{\text{Misclassified genuine in-air signatures}}{\text{Total number of genuine in-air signatures}} * 100 \quad (16)$$

- False Rejection Rate (FRR) is the probability that genuine in-air signatures are incorrectly rejected as forged in-air signatures by the system.

$$FRR = \frac{\text{Misclassified forgery in-air signatures}}{\text{Total number of forgery in-air signatures}} * 100 \quad (17)$$

- Equal Error Rate (EER)

To determine EER, we follow these steps:

1) We collect genuine and forged scores from the DTW using the template signature.

2) We sort the scores by arranging the genuine and forged scores in ascending order.

3) We define a range of decision thresholds that we'll evaluate. These thresholds represent the point at which similarity scores are considered a match or non-match.

4) We calculate the FRR and the FAR based on the number of genuine scores incorrectly rejected and forged scores incorrectly accepted, respectively.

5) We find the threshold at which the FRR equals the FAR. EER is the point at which our system's false rejection rate matches the false acceptance rate.

6) We report the EER which is typically expressed as a percentage and represents our system's overall performance.

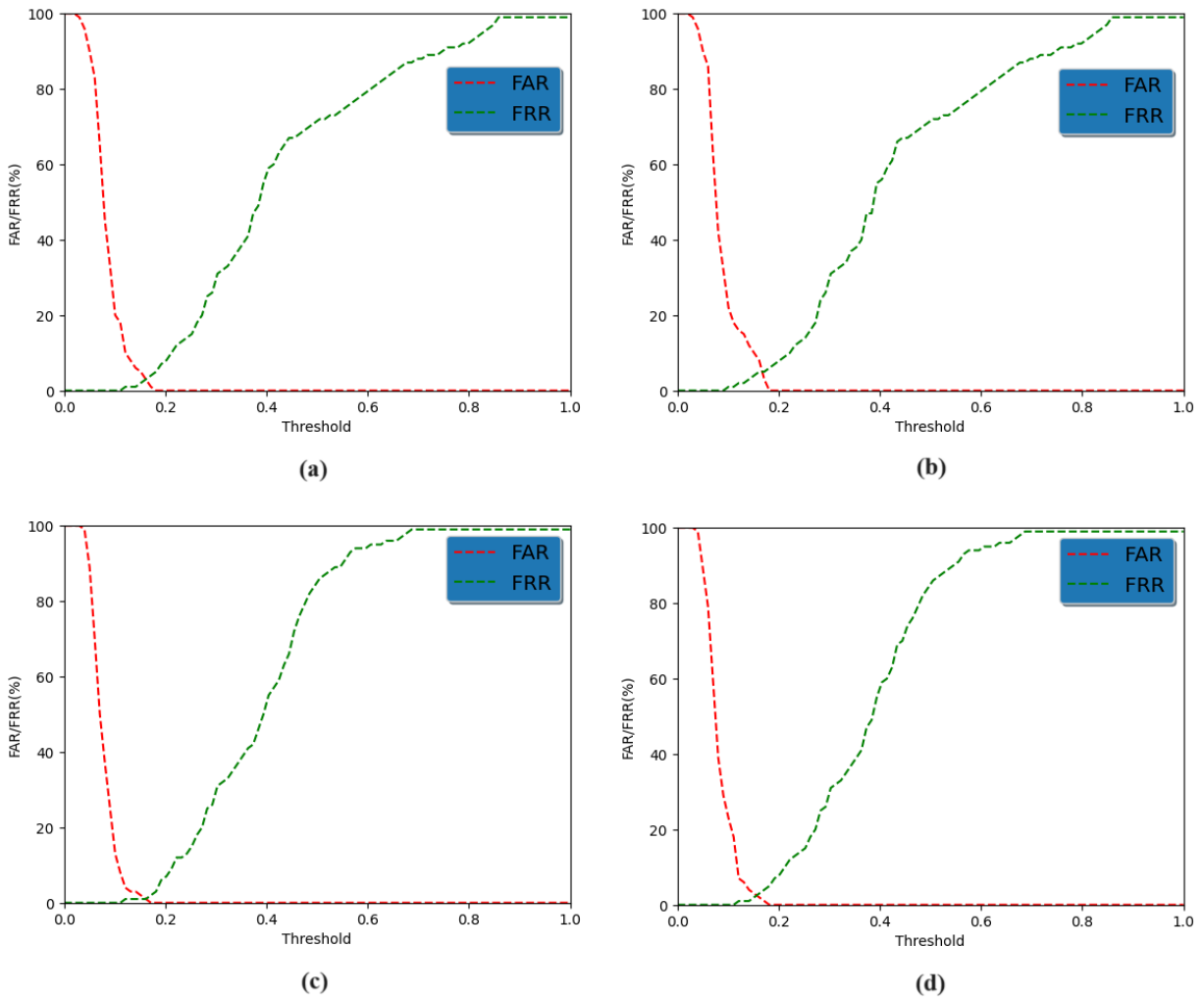


FIGURE 12. (a): Results using IAS dataset for the skilled-forgery scenario; (b): Results using IASGP dataset for the skilled-forgery scenario; (c): Results using IAS dataset for the random-forgery scenario; (d): Results using IASGP dataset for the random-forgery scenario.

Lower EER values indicate better performance, as they imply a smaller gap between the FRR and FAR.

The relationship between FAR, FRR and EER and the ROC curve are shown in Figure 11.

B. RESULTS AND DISCUSSION

To evaluate the effectiveness of our in-air signature verification system, we performed the experiments using our datasets, the 3DAirSig dataset [28] and the DeepAirSig dataset [23].

1) EXPERIMENTS ON OUR DATASETS

During the training of the forty users for both IAS and IASGP datasets, we randomly selected 3 genuine signatures for each signer as the reference set in each experiment. The remaining 2 genuine signatures and 5 skillfully forged signatures were used for the test samples as presented in Table 6.

TABLE 6. Enrollment protocol using IAS and IASGP datasets.

Phase	Signatures category	Signature type	Number of signatures
Train	Train signatures	Genuine	3
Test	Test signatures	Genuine	2
		Skilled forgeries	5

To prevent a selection bias, we repeated all the experiments five times in both IAS and IASGP datasets. Figure 12 (a, b) and Table 7 show the average in-air signature verification results of the proposed system on both IAS and IASGP datasets for the skilled-forgery scenario.

TABLE 7. Results using IAS and IASGP datasets for the skilled-forgery scenario.

Dataset	FAR (%)	FRR (%)	EER (%)
IAS dataset	2.00	1.00	1.25
IASGP dataset	4.25	1.25	2.00

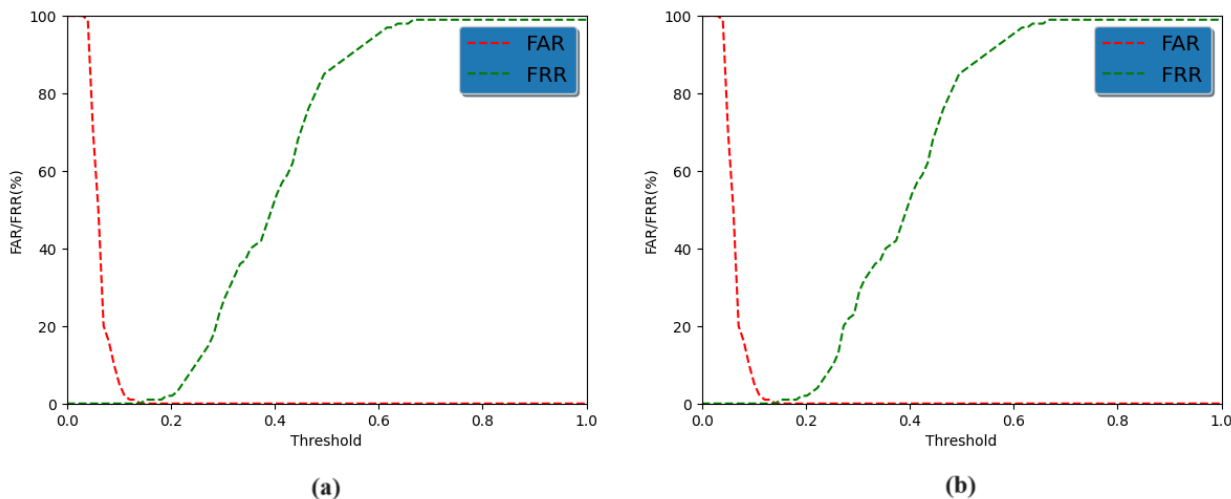


FIGURE 13. (a): Results using 3DAirSig dataset for the skilled-forgery scenario; (b): Results using 3DAirSig dataset for the random-forgery scenario.

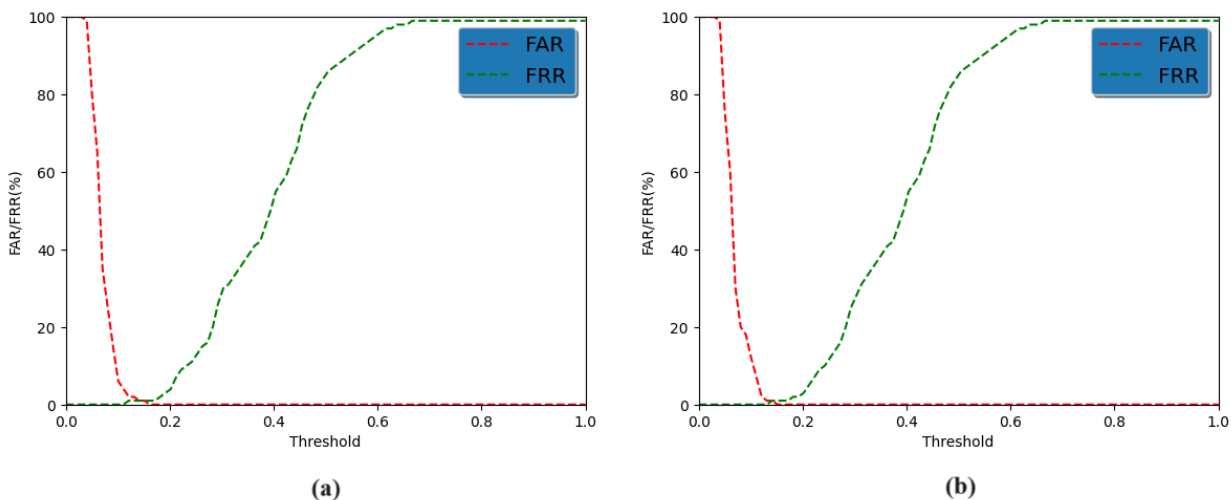


FIGURE 14. (a): Results using DeepAirSig dataset for the skilled-forgery scenario; (b): Results using DeepAirSig dataset for the random-forgery scenario.

The analysis of the results reveals that our proposed system, using the Beta-elliptical approach and the fuzzy perceptual detector in features extraction and the DTW in verification, is effective to distinguish between genuine and forged in-air signatures. It can be noted that the FAR in IAS and IASGP datasets belong to different users, which indicates that our proposed system has relatively low fault tolerance. As can be noticed also, the results of FRR in IAS dataset and IASGP dataset are inferior to 1.50%. In other words, we can say that our in-air signature verification system can detect a misclassified forgery with a good performance in the two cases with and without the use of a transparent glass plate.

We also observe that the results on IASGP dataset using the transparent glass plate give us an EER higher than the results on IAS dataset. This can be explained by the fact that IASGP

dataset is more challenging. In fact, the use of a transparent glass plate in IASGP dataset adds a constraint to the in-air signature, which can affect the quality of information of the in-air signature verification system.

Some of the anterior works studied not only the skilled-forgery scenario, but also the random-forgery scenario. For this reason, we conducted an experiment on random-forgery scenario. The random-forgery scores were achieved by comparing the selected template genuine signature to the two remaining genuine signatures from the target signer as genuine signatures and all the genuine signatures from each of the remaining signers as forged signatures in the verification phase. Figure 12 (c, d) and Table 8 show the in-air signature verification results of the proposed system on both IAS and IASGP datasets for the random-forgery scenario.

TABLE 8. Results using IAS and IASGP datasets for the random -forgery scenario.

Dataset	FAR (%)	FRR (%)	EER (%)
IAS dataset	1.50	0.25	0.76
IASGP dataset	2.25	0.75	1.23

TABLE 9. Enrollment protocol using 3DAirSig dataset.

Phase	Signatures category	Signature type	Number of signatures
Train	Train signatures	Genuine	5
Test	Test signatures	Genuine	10
		Skilled forgeries	25

From the obtained results, we can conclude that our proposed system is effective for in-air signature verification for both skilled-forgery and random-forgery scenarios.

2) EXPERIMENTS ON THE 3DAIRSIG DATASET

We made use of the publicly available dataset called 3DAirSig dataset created by Malik et al. [28] and which was contributed by 15 volunteers. For each volunteer, the dataset contained 5 genuine signatures as the reference set for the training and 10 genuine signatures and 25 skilled forgeries obtained from five impostors for the testing process as presented in Table 9.

TABLE 10. Results using 3DAirSig dataset for the skilled-forgery scenario.

System	FAR (%)	FRR (%)	EER (%)
Depth-based Signature verification method [28]	1.33	2.00	0.51
2D Spatial-based Signature Verification method [28]	2.93	5.33	0.69
Improved 2D Spatial-based Signature Verification method [28]	1.60	3.34	0.58
3D Signature Verification method [28]	0.80	2.00	0.46
Mean templates and DTW [24]	-	-	0.60
Mean templates and a weighted DTW (WDTW) [24]	-	-	0.10
Mean templates and sliding window dynamic time warping (SW-DTW) [24]	-	-	0.10
A novel single-template strategy using mean templates and DTW weighted by the local stability sequence [24]	-	-	0.00
Our System	0	0.18	0.08

Figure 13 (a) and Table 10 show the in-air signature verification results of the proposed system using 3DAirSig dataset for the skilled-forgery scenario. The analysis of the results reveals that our proposed system, using the Beta-elliptical approach and the fuzzy perceptual detector in features extraction and the DTW in verification, gives a comparative result, with an EER equal to 0.08, compared

to the work presented in [24]. This proves the effectiveness of the proposed system to distinguish between genuine and forged in-air signatures.

We also conducted the experiment on random-forgery scenario. The random-forgery scores were achieved by comparing the selected template genuine signature to the remaining 10 genuine signatures from the target signer as genuine signatures and all the genuine signatures from each of the remaining signers as forged signatures in the verification phase as in the protocol evaluation presented in [24]. Figure 13 (b) and Table 11 show the in-air signature verification results of the proposed system using 3DAirSig dataset for random-forgery.

TABLE 11. Results using 3DAirSig dataset for the random -forgery scenario.

System	FAR (%)	FRR (%)	ERR (%)
Mean templates and DTW [24]	-	-	0.57
Mean templates and a weighted DTW (WDTW) [24]	-	-	0.57
Mean templates and sliding window dynamic time warping (SW-DTW) [24]	-	-	0.57
A novel single-template strategy using mean templates and DTW weighted by the local stability sequence [24]	-	-	0.52
Our System	0	0.10	0.06

The results reveal that our proposed system outperforms the in-air signature verification systems presented in [24], suggesting that the Beta-elliptical approach and the fuzzy perceptual detector in features extraction serve as powerful tools for the in-air signature verification process.

3) EXPERIMENTS ON THE DEEPAIRSIG DATASET

We utilized also the publicly accessible DeepAirSig dataset, established by Malik et al. [23]. This dataset consisted of contributions from 40 volunteers. Within this dataset, each volunteer’s data included 10 genuine signatures for training as the reference set and 10 genuine signatures along with 25 skilled forgeries obtained from five impostors for the testing phase, as outlined in Table 12.

TABLE 12. Enrollment protocol using DeepAirSig dataset.

Phase	Signatures category	Signature type	Number of signatures
Train	Train signatures	Genuine	10
Test	Test signatures	Genuine	10
		Skilled forgeries	25

Figure 14 (a) and Table 13 show the in-air signature verification results of the proposed system using DeepAirSig dataset for the skilled-forgery scenario.

The analysis of the obtained results reveals that our proposed system, using the Beta-elliptical approach and the

TABLE 13. Results using DeepAirSig dataset for the skilled-forgery scenario.

System	FAR (%)	FRR (%)	ERR (%)
3D(X,Y,Z) and PointCloud-based verification [23]	-	-	0.05
Real data and synthetic 3D signatures from Sigma-Lognormal model with DTW verification [20]	-	-	1.91
The velocity, the acceleration and the position coordinates with DTW [21]	-	-	5.09
Our System	0.86	1.42	0.34

fuzzy perceptual detector in features extraction and the DTW in verification, gives a comparative result, with an EER equal to 0.34%.

We additionally carried out an experiment under a random-forgery scenario. In this scenario, the random-forgery scores were obtained by comparing the selected template genuine signature to the remaining 10 genuine signatures from the target signer considered as genuine, and all the genuine signatures from each of the other signers were treated as forged during the verification phase. The results of the in-air signature verification using the DeepAirSig dataset for the random-forgery scenario are presented in Figure 14 (b) and Table 14.

TABLE 14. Results using DeepAirSig dataset for the random-forgery scenario.

System	FAR (%)	FRR (%)	EER (%)
Real data and synthetic 3D signatures from Sigma-Lognormal model with DTW verification [20]	-	-	0.27
The velocity, the acceleration and the position coordinates with DTW [21]	-	-	0.69
Our System	0.17	0.70	0.23

The results we acquired indicate that our proposed system surpasses the performance of the in-air signature verification systems introduced in [20] and [21]. This suggests that the utilization of the Beta-elliptical approach and the fuzzy perceptual detector in feature extraction demonstrates their effectiveness in the in-air signature verification process.

By utilizing a diverse dataset and implementing state-of-the-art techniques, the system is capable of recognizing subtle nuances in signature dynamics, ensuring reliable verification even in challenging real-world scenarios.

4) ANALYSIS OF VERTICAL DIMENSION VALUES OF THE IN-AIR SIGNATURES LINES

During the preprocessing phase, specifically within the normalization process, we conducted numerous experiments. These experiments involved varying the vertical dimension h of the in-air signature lines, as illustrated in Figure 15.

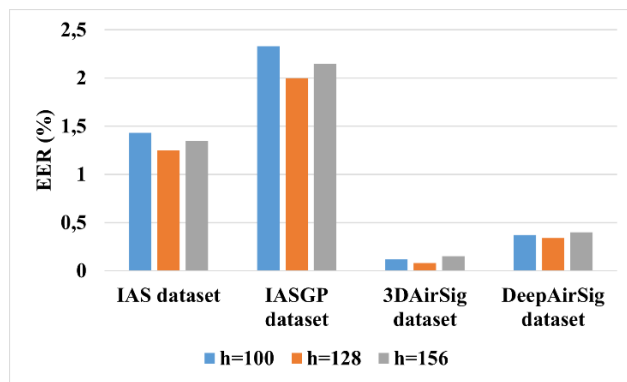


FIGURE 15. Equal Error Rate results using different vertical dimension h of the in-air signatures lines.

As depicted in Figure 15, the lowest EER is achieved when the value of h is set to 128.

VI. CONCLUSION AND FUTURE WORKS

A novel in-air signature verification system is proposed based on the Beta-elliptical approach and the fuzzy perceptual detector. DTW is used in verification. To evaluate the proposed system, two in-air signature datasets are created. Forty voluntary participants took part in both of the two datasets' construction. Experimental results indicate that our proposed system using the Beta-elliptical approach and the fuzzy perceptual detector in features extraction and DTW in verification is effective to distinguish between genuine and forged in-air signatures. The effectiveness of our proposed system was also examined using both the 3DAirSig and the DeepAirSig datasets, which achieves interesting results compared to those of the existing systems for both skilled-forgery and random-forgery scenarios. Our proposed system can be used in many applications like mail voting, access controls, official communications, forensic analysis, banking services and secure communication with IoT Devices.

The exploration of other alternative techniques for improving features extraction like the use of Jerk, which represents the time rate of change of acceleration, is planned in the next experimentations. Moreover, there are potential applications of the proposed method outside the e-security domain like the diagnosis of Parkinson's disease using in-air signatures.

DECLARATION

Financial Interests: The authors declare they have no financial interests.

Non-Financial Interests: None.

Conflict of Interest: The authors declare that they have no conflict of interest.

REFERENCES

[1] D. Impedovo and G. Pirlo, "Automatic signature verification: The state of the art," *IEEE Trans. Syst., Man, Cybern. C, Appl. Rev.*, vol. 38, no. 5, pp. 609-635, Sep. 2008, doi: 10.1109/TSMCC.2008.923866.

- [2] O. Kanich, J. Matejka, E. Fialová, M. P. Kafková, T. Doseděl, and M. Drahanský, "Technological, legal, and sociological summary of biometric technology usage," *ScienceOpen Res.*, Nov. 2022, pp. 1–7, doi: [10.14293/S2199-1006.1.SOR.2022.0002.v1](https://doi.org/10.14293/S2199-1006.1.SOR.2022.0002.v1).
- [3] H. Kaur and M. Kumar, "Signature identification and verification techniques: State-of-the-art work," *J. Ambient Intell. Humanized Comput.*, vol. 14, no. 2, pp. 1027–1045, Feb. 2023, doi: [10.1007/s12652-021-03356-w](https://doi.org/10.1007/s12652-021-03356-w).
- [4] R. Acosta-Velasquez, L. Espinosa-Leal, A. Garcia-Perez, and K.-M. Björk, "Verification of static signatures using dynamic time warping on features from high pressure points," in *Proc. Int. Conf. Extreme Learning Mach.*, K.-M. Björk, Ed. Cham, Switzerland: Springer, 2023, pp. 104–113, doi: [10.1007/978-3-031-21678-7_10](https://doi.org/10.1007/978-3-031-21678-7_10).
- [5] J. Long, C. Xie, and Z. Gao, "High discriminant features for writer-independent online signature verification," *Multimedia Tools Appl.*, vol. 82, no. 25, pp. 38447–38465, Mar. 2023, doi: [10.1007/s11042-023-14638-0](https://doi.org/10.1007/s11042-023-14638-0).
- [6] D. Mazzolini, P. Mignone, P. Pavan, and G. Vessio, "An easy-to-explain decision support framework for forensic analysis of dynamic signatures," *Forensic Sci. Int., Digit. Invest.*, vol. 38, Sep. 2021, Art. no. 301216, doi: [10.1016/j.fsidi.2021.301216](https://doi.org/10.1016/j.fsidi.2021.301216).
- [7] M. Houtinezhad and H. R. Ghaffari, "Off-line signature verification system using features linear mapping in the candidate points," *Multimedia Tools Appl.*, vol. 81, no. 17, pp. 24815–24847, Mar. 2022, doi: [10.1007/s11042-022-12499-7](https://doi.org/10.1007/s11042-022-12499-7).
- [8] T. Dhieb, H. Boubaker, S. Njah, M. Ben Ayed, and A. M. Alimi, "A novel biometric system for signature verification based on score level fusion approach," *Multimedia Tools Appl.*, vol. 81, no. 6, pp. 7817–7845, Mar. 2022, doi: [10.1007/s11042-022-12140-7](https://doi.org/10.1007/s11042-022-12140-7).
- [9] S. Kanakaprabha, P. Arulprakash, V. Priyanka, V. Varghese, and A. Sureshkumar, "IoT based solution for effective social distancing and contact tracing for COVID-19 prevention," in *Intelligent Cyber Physical Systems and Internet of Things*, J. Hemanth, D. Pelusi, and J. L.-Z. Chen, Eds. Cham, Switzerland: Springer, 2023, pp. 629–643, doi: [10.1007/978-3-031-18497-0_46](https://doi.org/10.1007/978-3-031-18497-0_46).
- [10] G. Li and H. Sato, "Sensing in-air signature motions using smartwatch: A high-precision approach of behavioral authentication," *IEEE Access*, vol. 10, pp. 57865–57879, 2022, doi: [10.1109/ACCESS.2022.3177905](https://doi.org/10.1109/ACCESS.2022.3177905).
- [11] A. Q. Ansari, M. Hanmandlu, J. Kour, and A. K. Singh, "Online signature verification using segment-level fuzzy modelling," *IET Biometrics*, vol. 3, no. 3, pp. 113–127, Sep. 2014, doi: [10.1049/iet-bmt.2012.0048](https://doi.org/10.1049/iet-bmt.2012.0048).
- [12] F. Zhang, V. Bazarevsky, A. Vakunov, A. Tkachenka, G. Sung, C.-L. Chang, and M. Grundmann, "MediaPipe hands: On-device real-time hand tracking," 2020, *arXiv:2006.10214*.
- [13] T. Dhieb, H. Boubaker, W. Ouarda, S. Njah, M. Ben Ayed, and A. M. Alimi, "Deep bidirectional long short-term memory for online multilingual writer identification based on an extended beta-elliptical model and fuzzy elementary perceptual codes," *Multimedia Tools Appl.*, vol. 80, no. 9, pp. 14075–14100, Apr. 2021, doi: [10.1007/s11042-020-10412-8](https://doi.org/10.1007/s11042-020-10412-8).
- [14] H. Boubaker, A. Chaabouni, N. Tagougui, M. Kherallah, and A. M. Alimi, "Handwriting and hand drawing velocity modeling by superposing beta impulses and continuous training component," *Int. J. Comput. Sci. Issues*, vol. 10, no. 5, p. 7, 2013.
- [15] S. Njah, M. Ltaief, H. Bezine, and A. M. Alimi, "The PerTOHS theory for F or on-line on line handwriting segmentation," *Int. J. Comput. Sci. Issues*, vol. 9, no. 5, p. 142, 2012.
- [16] S. Njah, H. Bezine, and A. M. Alimi, "On-line Arabic handwriting segmentation via perceptual codes: Application to MAYASTROUN database," in *Proc. 8th Int. Multi-Conf. Syst., Signals Devices*, Mar. 2011, pp. 1–5, doi: [10.1109/SSD.2011.5993564](https://doi.org/10.1109/SSD.2011.5993564).
- [17] H. S. Kang, I. S. Koh, K. Makimoto, and M. Yamakawa, "Nurses' perception towards care robots and their work experience with socially assistive technology during COVID-19: A qualitative study," *Geriatric Nursing*, vol. 50, pp. 234–239, Mar. 2023, doi: [10.1016/j.gerinurse.2023.01.025](https://doi.org/10.1016/j.gerinurse.2023.01.025).
- [18] V. Munasinghe, Y.-M. Li, T. S. Kim, and H.-J. Lee, "CNN-based hand gesture recognition for contactless elevator button control," in *Proc. Int. Conf. Electron., Inf., Commun. (ICEIC)*, Feb. 2023, pp. 1–2, doi: [10.1109/ICEIC57457.2023.10049968](https://doi.org/10.1109/ICEIC57457.2023.10049968).
- [19] C. T. Lee and L.-Y. Pan, "Smile to pay: Predicting continuous usage intention toward contactless payment services in the post-COVID-19 era," *Int. J. Bank Marketing*, vol. 41, no. 2, pp. 312–332, Mar. 2023, doi: [10.1108/ijbm-03-2022-0130](https://doi.org/10.1108/ijbm-03-2022-0130).
- [20] M. A. Ferrer, M. Diaz, C. Carmona-Duarte, J. J. Quintana, and R. Plamondon, "Synthesis of 3D on-air signatures with the Sigma-Lognormal model," *Knowl.-Based Syst.*, vol. 265, Apr. 2023, Art. no. 110365, doi: [10.1016/j.knsys.2023.110365](https://doi.org/10.1016/j.knsys.2023.110365).
- [21] M. Diaz, M. A. Ferrer, C. Carmona-Duarte, J. J. Quintana, A. Morales, J. Fierrez, and R. Plamondon, "Kinematic synthesis for 3D signatures," in *Proc. IEEE Int. Joint Conf. Biometrics (IJCB)*, Oct. 2022, pp. 1–7, doi: [10.1109/IJCB54206.2022.10007945](https://doi.org/10.1109/IJCB54206.2022.10007945).
- [22] W. H. Khoh, Y. H. Pang, and H. Y. Yap, "In-air hand gesture signature recognition: An iHGS database acquisition protocol," *FResearch*, vol. 11, p. 283, Mar. 2022, doi: [10.12688/f1000research.74134.1](https://doi.org/10.12688/f1000research.74134.1).
- [23] J. Malik, A. Elhayek, S. Guha, S. Ahmed, A. Gillani, and D. Stricker, "DeepAirSig: End-to-end deep learning based in-air signature verification," *IEEE Access*, vol. 8, pp. 195832–195843, 2020, doi: [10.1109/ACCESS.2020.3033848](https://doi.org/10.1109/ACCESS.2020.3033848).
- [24] M. Okawa, "Time-series averaging and local stability-weighted dynamic time warping for online signature verification," *Pattern Recognit.*, vol. 112, Apr. 2021, Art. no. 107699, doi: [10.1016/j.patcoc.2020.107699](https://doi.org/10.1016/j.patcoc.2020.107699).
- [25] W. H. Khoh, Y. H. Pang, A. B. J. Teoh, and S. Y. Ooi, "In-air hand gesture signature using transfer learning and its forgery attack," *Appl. Soft Comput.*, vol. 113, Dec. 2021, Art. no. 108033, doi: [10.1016/j.asoc.2021.108033](https://doi.org/10.1016/j.asoc.2021.108033).
- [26] E. Guerra-Segura, A. Ortega-Pérez, and C. M. Travieso, "In-air signature verification system using leap motion," *Expert Syst. Appl.*, vol. 165, Mar. 2021, Art. no. 113797, doi: [10.1016/j.eswa.2020.113797](https://doi.org/10.1016/j.eswa.2020.113797).
- [27] W. H. Khoh, Y. H. Pang, and A. B. J. Teoh, "In-air hand gesture signature recognition system based on 3-dimensional imagery," *Multimedia Tools Appl.*, vol. 78, no. 6, pp. 6913–6937, Mar. 2019, doi: [10.1007/s11042-018-6458-7](https://doi.org/10.1007/s11042-018-6458-7).
- [28] J. Malik, A. Elhayek, S. Ahmed, F. Shafait, M. Malik, and D. Stricker, "3DAirSig: A framework for enabling in-air signatures using a multimodal depth sensor," *Sensors*, vol. 18, no. 11, p. 3872, Nov. 2018, doi: [10.3390/s18113872](https://doi.org/10.3390/s18113872).
- [29] Y. Fang, W. Kang, Q. Wu, and L. Tang, "A novel video-based system for in-air signature verification," *Comput. Electr. Eng.*, vol. 57, pp. 1–14, Jan. 2017, doi: [10.1016/j.compeleceng.2016.11.010](https://doi.org/10.1016/j.compeleceng.2016.11.010).
- [30] H. Bezine, A. M. Alimi, and N. Derbel, "Handwriting trajectory movements controlled by a beta-elliptical model," in *Proc. 7th Int. Conf. Document Anal. Recognit.*, Aug. 2003, p. 1228.
- [31] A. M. Alimi, "An evolutionary neuro-fuzzy approach to recognize on-line Arabic handwriting," in *Proc. 4th Int. Conf. Document Anal. Recognit.*, Aug. 1997, pp. 382–386, doi: [10.1109/ICDAR.1997.619875](https://doi.org/10.1109/ICDAR.1997.619875).
- [32] P. Viviani and R. Schneider, "A developmental study of the relationship between geometry and kinematics in drawing movements," *J. Experim. Psychol., Hum. Perception Perform.*, vol. 17, no. 1, pp. 198–218, 1991, doi: [10.1037/0096-1523.17.1.198](https://doi.org/10.1037/0096-1523.17.1.198).
- [33] M. B. Abdallah, M. Kallel, and M. S. Bouhlel, "An overview of gesture recognition," in *Proc. 6th Int. Conf. Sci. Electron., Technol. Inf. Telecommun. (SETIT)*, Mar. 2012, pp. 20–24, doi: [10.1109/SETIT.2012.6481883](https://doi.org/10.1109/SETIT.2012.6481883).
- [34] X. Wang, X. Zhao, and Y. Zhang, "Deep-learning-based reading eye-movement analysis for aiding biometric recognition," *Neurocomputing*, vol. 444, pp. 390–398, Jul. 2021, doi: [10.1016/j.neucom.2020.06.137](https://doi.org/10.1016/j.neucom.2020.06.137).
- [35] I. Zacharakis and D. Giagopoulos, "Model-based damage localization using the particle swarm optimization algorithm and dynamic time wrapping for pattern recreation," *Sensors*, vol. 23, no. 2, p. 591, Jan. 2023, doi: [10.3390/s23020591](https://doi.org/10.3390/s23020591).



ABDULAZEEZ R. ALOBAIDI was born in Amara, Iraq, in 1988. He received the master's degree in computer science "information technologies" from UNITAR International University, in 2014. He is currently pursuing the Ph.D. degree in computer science with the National School of Engineers of Sfax, Tunisia. His main research interests include deep-air signature identification and verification systems. He is a member of the Research Groups in Intelligent Machines—REGIM Laboratory, Enis, University of Sfax, Tunisia.



THAMEUR DHIEB (Member, IEEE) was born in Sfax, Tunisia, in 1985. He received the M.S. degree in computer science from FSEGS, Tunisia, in 2012, and the Ph.D. degree in computer science from ISITCOM, Tunisia, in 2021. He is currently an Assistant Professor with the Higher Institute of Business Administration of Gafsa. His research interests include writer identification and signature verification. He is a Reviewer of IEEE Access, *Neurocomputing*, *Expert Systems with Applications*, *Cognitive Computation*, and *Egyptian Informatics Journal*. He is affiliated with the Research Groups in Intelligent Machines—REGIM Laboratory, Enis, University of Sfax, Tunisia.



TAREK M. HAMDANI (Senior Member, IEEE) was born in Tunis, Tunisia, in 1979. He received the M.Sc., Ph.D., and H.D.R. degrees in computer science engineering from the National Engineering School of Sfax, Tunisia, in 2003, 2011, and 2019, respectively. He is currently an Associate Professor in computer science with the University of Monastir, Monastir. His research interests include applying intelligent methods (neural networks, fuzzy logic, and evolutionary algorithms) to machine learning, computer vision, natural language processing, intelligent pattern recognition, and analysis of large scale complex systems. He is a Senior Member of CIS and SMC Societies. He is a Reviewer of the *Pattern Recognition Letters*, *Neurocomputing*, *Neural Processing Letter*, IEEE TRANSACTIONS ON NEURAL NETWORKS AND LEARNING SYSTEMS, and the *Soft Computing* journal.



ALI WALI (Senior Member, IEEE) received the Ph.D. degree in engineering computer systems from the National School of Engineers of Sfax, in 2013. He is currently an Associate Professor in signal and image processing with ISIM, University of Sfax. He is also a member of the REsearch Groups on Intelligent Machines (REGIM Laboratory). His research interests include computer vision and image and video analysis, video events detection, and pattern recognition. He was a member of the Organizing Committee of the International Conference on Machine Intelligence ACIDCA-ICMI2005, the Third IEEE International Conference on Next Generation Networks and Services (NGNS2011), the Fourth International Conference on Logistics (LOGISTIQUA2011), the International Conference on Advanced Logistics and Transport (ICALT'2013, ICALT'2014, and ICALT'2015), the 13th International Conference on Document Analysis and Recognition (ICDAR 2015), the International Conference on Hybrid Intelligent Systems (HIS'2013), and the International Conference on Information Assurance and Security (IAS'2013).



KHMAIES OUAHADA (Senior Member, IEEE) received the B.Eng. degree from the University of Khartoum, Sudan, in 1995, and the M.Eng. (Hons.) and D.Eng. degrees from the University of Johannesburg, South Africa, in 2002 and 2009, respectively. He was with Sudatel—the Sudanese National Communications Company. He is currently the former HOD (2019–2021). He is also a Professor with the University of Johannesburg, where he is also the Founder and the Deputy Director of the Centre for Smart Information and Communications Systems research group, Faculty of Engineering and the Built Environment. He is also a Rated Researcher with the National Research Foundation of South Africa. His research interests include information theory, coding techniques, power-line communications, visible light communication, smart grids, energy demand management, renewable energy, wireless sensor networks, the IoT, reverse engineering, and engineering education. He is a Senior Member of the IEEE Information Theory and Communications Societies and the SAIEE Society.



ADEL M. ALIMI (Senior Member, IEEE) was born in Sfax, Tunisia, in 1966. He received the degree in electrical engineering, in 1990, and the Ph.D. and H.D.R. degrees in electrical and computer engineering, in 1995 and 2000, respectively. He is currently a Professor in electrical and computer engineering with the University of Sfax. His research interests include the applications of intelligent methods (neural networks, fuzzy logic, and evolutionary algorithms) to pattern recognition, robotic systems, vision systems, industrial processes, intelligent pattern recognition, learning, analysis, and intelligent control of large-scale complex systems. He is the Founder and the Chair of many IEEE Chapter in Tunisia Section. He is also the IEEE Sfax Subsection Chair, in 2011, the IEEE ENIS Student Branch Counselor, in 2011, the IEEE Systems, Man, and Cybernetics Society Tunisia Chapter Chair, in 2011, and the IEEE Computer Society Tunisia Chapter Chair, in 2011. He is also an Expert Evaluator of the European Agency for Research. He was the General Chairperson of the International Conference on Machine Intelligence ACIDCA-ICMI'2005 and ACIDCA-ICMI'2000. He is also an Associate Editor and a member of the Editorial Board of many international scientific journals, such as IEEE TRANSACTIONS ON FUZZY SYSTEMS, *Neurocomputing*, *Neural Processing Letters*, *International Journal of Image and Graphics*, *Neural Computing and Applications*, *International Journal of Robotics and Automation*, and *International Journal of Systems Science*. He was a Guest Editor of several special issues of international journals, such as *Fuzzy Sets and Systems*, *Soft Computing*, *Journal of Decision Systems*, *Integrated Computer-Aided Engineering*, and *Systems Analysis Modeling Simulation*.

...